



Multi-response optimisation of the solar photo-Fenton process for landfill leachate post-treatment

Larissa Granjeiro Lucena^{a,*}, Elisângela Maria Rodrigues Rocha^a,
Camila de Almeida Porto^a, Nathália Aquino de Carvalho^a,
Flávio Luiz Honorato da Silva^b

^aDepartment of Civil and Environmental Engineering, Universidade Federal da Paraíba, Cidade Universitária, João Pessoa, PB 58051–900, Brazil, Tel. +55 83 3216 7119; Fax: +55 83 3216 7179; emails: larissalucena05@gmail.com (L.G. Lucena), elis_eng@yahoo.com.br (E.M.R. Rocha), camila.aporto@hotmail.com (C. de Almeida Porto), nathalia_aq@hotmail.com (N. Aquino de Carvalho)

^bDepartment of Chemical Engineering, Universidade Federal da Paraíba, Cidade Universitária, João Pessoa, PB 58051–900, Brazil, email: flavioluizh@yahoo.com.br (F.L. Honorato da Silva)

Received 16 April 2018; Accepted 5 January 2019

ABSTRACT

In this study, central composite design (CCD) and response surface methodology (RSM) were applied to assess and optimise the solar photo-Fenton process ($\text{Fe}^{2+}/\text{H}_2\text{O}_2/\text{solar UV}$) used as a post-treatment for a leachate from a landfill stabilisation lagoon system in João Pessoa, Brazil. Three variables were investigated: hydrogen peroxide (H_2O_2) factor, reagents ratio $[\text{H}_2\text{O}_2]/[\text{FeSO}_4]$ and initial pH of the reaction. The objectives were to maximise the removal of chemical oxygen demand (COD), turbidity and colour, and to minimise sludge generation in terms of settleable and total solids. According to the analysis of variance (ANOVA), all the response models using the selected variables were statistically significant, with determination coefficient (R^2) varying between 0.756 and 0.976. The optimal operational ranges were determined by overlaying contour plots: 0.83–1.50 (H_2O_2 factor), 3.70–5.40 (reagents ratio), and 2.72–3.15 (pH). The contour plots defined by the models showed strong interactions between the variables, whose values must meet the optimal ranges established in the study and follow these interactions to achieve COD removal >75%, turbidity removal >90%, colour removal >97%, generation of settleable solids <60 $\text{mL}\cdot\text{L}^{-1}$ and generation of total solids <50 $\text{mg}\cdot\text{L}^{-1}$. The validation tests proved an excellent fit of the model to the experimental data. Finally, it was demonstrated that the solar photo-Fenton process was effective as a post-treatment for a mature landfill leachate, and its optimisation improved the quality of the final effluent.

Keywords: Landfill leachate; Solar photo-Fenton process; Advanced oxidative processes (AOPs); Central composite design (CCD); Response surface methodology (RSM); Sludge reduction

1. Introduction

Landfills are one of the most widely used methods to manage municipal solid waste [1]. In this approach, the combination of physical, chemical and microbiological processes transfers pollutants from the solid waste to the percolation water, generating landfill leachates [2]. In general, this results

in a complex aqueous matrix with four groups of main pollutants [3]: (i) dissolved organic matter, (ii) inorganic macro components, (iii) metals, and (iv) xenobiotic organic compounds. These pollutants can induce severe adverse environmental impacts such as soil pollution, contamination of surface water and groundwater, and cause genetic disorders in animals [4–6]. Thus, various techniques are being

* Corresponding author.

researched as alternatives to remove such pollutants, including combined treatment with domestic sewage, aerobic and anaerobic biological treatments, chemical and physical processes (flotation, coagulation/flocculation, adsorption, chemical precipitation, ammonia stripping, ion exchange, chemical and electrochemical oxidation), membrane filtration (microfiltration, ultrafiltration, nanofiltration and reverse osmosis) and advanced oxidative processes (AOPs) [7–12].

AOPs have received great attention in the last two decades because of their capability to degrade recalcitrant molecules to biodegradable compounds or even to completely mineralise them to CO_2 , H_2O and inorganic ions [13,14]. Among the AOPs, the photo-Fenton process ($\text{Fe}^{2+}/\text{H}_2\text{O}_2/\text{UV}$) is a homogeneous photocatalytic process with a high efficiency to generate radicals that oxidise organic matter (hydroxyl radicals – $\text{OH}\bullet$) through the decomposition of hydrogen peroxide (H_2O_2) catalysed by ferrous ions (Fe^{2+}), under acidic conditions in the presence of natural or artificial ultraviolet-visible radiation (UV-VIS; $\lambda < 600 \text{ nm}$) [15]. The photolysis of Fe^{3+} complexes promotes Fe^{2+} regeneration [16], which favours the generation rate of $\text{OH}\bullet$ radicals. In addition, the efficiency of the photo-Fenton process compared with those of other AOPs has been demonstrated, such as in a study performed by Primo, Rivero and Ortiz [17], which analyses the efficiency of several AOPs in terms of COD removal from landfill leachates and defines the following relation, from least efficient to most efficient: $\text{UV} < \text{UV}/\text{H}_2\text{O}_2 < \text{Fenton} (\text{Fe}^{2+}/\text{H}_2\text{O}_2) < \text{Fenton-like} (\text{Cu}^{2+}/\text{H}_2\text{O}_2) < \text{photo-Fenton} (\text{UV}/\text{Fe}^{2+}/\text{H}_2\text{O}_2)$. Rocha et al. [18] and Starling et al. [19] have affirmed that AOPs are even more economically attractive when solar energy is used as a source of UV photons.

In this context, the study of variables that may interfere with the photo-Fenton process is essential to achieve the ideal operational conditions, aiming to maximise treatment efficiency and minimise sludge generation as a by-product. The main variables of the photo-Fenton process are the reagents' conditions – the ratios of ferrous [Fe^{2+}] and ferric [Fe^{3+}] ions and hydrogen peroxide [H_2O_2] – and the reaction characteristics (pH, radiation flux, temperature and

amounts of organic and inorganic constituents) [13]. When a combination of several variables and their interactions are considered, the response surface methodology (RSM) is a recognised tool for process design and optimisation with minimum experimental test numbers [20]. In addition, the optimisation of experimental variables for various responses could be done by overlaying critical responses on a single contour curve [21].

Although, there are relevant optimisation studies of the Fenton process performed with RSM [22–31], only few studies available mention the optimisation of the photo-Fenton process being applied to leachate treatment by RSM application [32]. Hence, the objective of this research was to study the optimal conditions of the solar photo-Fenton process applied to the post-treatment of a mature and recalcitrant leachate from the system of stabilisation lagoons of the municipal landfill of João Pessoa (Brazil). The optimisation was aimed to maximise COD, colour and turbidity removal, and to minimise sludge generation based on the analysis of total and settleable solids.

2. Materials and methods

2.1. Characteristics of the landfill leachate

Leachate samples were collected after biological treatment in the landfill stabilisation lagoons. The landfill is located at the metropolitan area of João Pessoa, Northeast Brazil, and has operated since 2003. Samples were sent to the laboratory at the Federal University of Paraíba (UFPB) and stored at 4°C . Table 1 shows the physical and chemical characteristics of the leachate used in this study, designated as raw leachate. Analyses were performed according to Standard Methods for the Examination of Water and Wastewater [33].

The leachate is an alkaline effluent, dark brown in colour, mature (>10 years old), stabilised, and of low biodegradability (BOD_5/COD equal to 0.22). These characteristics indicate the need for advanced treatment.

Table 1
Characterisation of the landfill leachate

Parameter	Lo ^a		Lv ^b		Method code
	Value	<i>n</i>	Value	<i>n</i>	
pH	7.6 ± 0.0	3	7.4 ± 0.1	3	4500-H ⁺ B
Turbidity, NTU	293.0 ± 0.6	3	143.0 ± 1.0	3	2130 B
Conductivity, $\text{mS}\cdot\text{cm}^{-1}$	5.8 ± 0.0	2	15.6 ± 0.0	2	2510 B
Alkalinity, $\text{mg CaCO}_3\cdot\text{L}^{-1}$	3,950.0 ± 35.4	2	5,750.0 ± 0.0	2	2320 B
Chlorides, $\text{mg Cl}^{-}\cdot\text{L}^{-1}$	3,173.6 ± 35.1	3	2,280.0 ± 70.1	3	4500-Cl ⁻ B
BOD_5 , $\text{mg O}_2\cdot\text{L}^{-1}$	448.0 ± 11.0	3	494.0 ± 7.1	2	5210 D
COD, $\text{mg O}_2\cdot\text{L}^{-1}$	2,038.4 ± 39.2	3	2,388.6 ± 17.7	2	5220 D
Total solids, $\text{mg}\cdot\text{L}^{-1}$	7,610.0	1	10,023.3	1	2540 G
Total volatile solids, $\text{mg}\cdot\text{L}^{-1}$	1,783.3	1	2,393.3	1	2540 G
Total fixed solids, $\text{mg}\cdot\text{L}^{-1}$	5,826.7	1	7,630.0	1	2540 G

^aLo: Leachate samples used in the optimisation process.

^bLv: Leachate samples used in the experimental validation.

2.2. Experimental design and statistical model

Central composite design (CCD) and RSM were applied to analyse the data and optimise the interfering variables of the solar photo-Fenton process: H_2O_2 factor, $[H_2O_2]/[FeSO_4]$ ratio and initial pH. The theoretical mass ratio for removal of COD through H_2O_2 was $1,000/470.6 = 2.125$. That is, $1,000 \text{ mg}\cdot\text{L}^{-1}$ of H_2O_2 theoretically removes $470.6 \text{ mg}\cdot\text{L}^{-1}$ of COD by oxidation [34]. Therefore, the calculation of the theoretical concentration of H_2O_2 is presented in Eq. (1):

$$[H_2O_2] = H_2O_2 \text{ factor} \times 2.125 \times COD_{\text{raw leachate}} \quad (1)$$

where H_2O_2 factor is the multiplying factor corresponding to the percentage of the H_2O_2 quantity relative to the stoichiometric quantity of O_2 needed to totally stabilise COD [35].

The values of the variables were chosen based on the literature [17,28,30,34,36,37]. The responses were defined based on the treatment goals: organic matter degradation in terms of COD (relevant response, also used by Ghanbarzadeh Lak et al. [26]; Amiri and Sabour [29]; Talebi et al. [27]; Erkan and Apaydin [30]); removal of suspended and dissolved solids in terms of turbidity and colour, respectively; and minimisation of sludge generation measured as settleable and total solids. Table 2 summarises the coded levels, the minimum (−1) and maximum (+1) factorial points, the minimum (−1.68) and maximum (+1.68) axial points, and the central point (0), as well as the respective decoded values of the three variables in the factorial design. A total of 18 tests were performed, eight in the full factorial design, six at the axial points, and four at the central point. The variables were in the following ranges: H_2O_2 factor between 0.33 and 1.67, $[H_2O_2]/[FeSO_4]$ ratio between 0.64 and 7.36, and initial pH between 2.16 and 3.84.

The experimental data were statistically analysed through the RSM procedure in the Statistica software (version 5.0, StatSoft) and fitted to an empirical second order polynomial model, as shown in Eq. (2) [21]:

$$Y = \beta_0 + \sum_{i=1}^k \beta_i X_i + \sum_{i=1}^k \beta_{ii} X_i^2 + \sum_{i < j=2}^k \sum_{i=1}^k \beta_{ij} X_i X_j + \varepsilon \quad (2)$$

where Y is the response; β_0 is the intercept constant, β_i is the coefficient of the first order term of factor i , β_{ii} is the coefficient of the quadratic term of factor i , and β_{ij} is the interaction coefficient between factors i and j . X_i and X_j are the decoded values of the factors, k is the number of variables, and ε is the residue.

Table 2
Variation levels of photo-Fenton process variables in the 2³ central composite designs

Experimental variable	Symbol	Coded and decoded variables				
		−1.68	−1	0	1	1.68
H_2O_2 factor	X_1	0.33	0.6	1.0	1.4	1.67
$[H_2O_2] / [FeSO_4]$	X_2	0.64	2.0	4.0	6.0	7.36
pH	X_3	2.16	2.5	3.0	3.5	3.84

The terms of the model were selected or rejected based on a P-value of a 95% confidence level. The results were statistically analysed by analysis of variance (ANOVA). The quality of the fit of the model to the experimental responses was expressed by the determination coefficient R^2 and adjusted R^2 , and its statistical significance was checked by the Fisher's F-test.

2.3. Simultaneous optimisation of the responses and optimal conditions

The optimal operational region of the variables that interfere with the solar photo-Fenton process (Fe^{2+}/H_2O_2 /solar UV) was obtained from the contour plots generated by the Statistica software, post-edited in the Adobe Illustrator CS6 software, by overlaying the contour plots considering the optimisation criteria of the selected responses (Table 3).

Contour plots are one of the most relevant ways to illustrate and explain response surfaces. They consist of bi-dimensional graphs (sometimes tri-dimensional) that show constant response contours (with an axis system that corresponds to specific pairs of experimental variables, X_i and X_j), while other variables are kept constant [21]. In this study, the values of the variables that were kept fixed were defined based on their meeting the limits established for each response, as shown in Table 3.

2.4. Experimental procedures

All the reagents used in the experiments were of analytical quality. First, heptahydrate ferrous sulphate ($FeSO_4 \cdot 7H_2O$, 99%, Vetec) was added to a beaker and diluted with 5 mL of distilled water [34]. Then, 200 mL of the sample of acidified leachate was added. The pH was previously adjusted with sulphuric acid (H_2SO_4 , 98%, Química Moderna) and a 6 M sodium hydroxide solution (NaOH, Química Moderna). The defined amount of H_2O_2 solution (30% v/v, Química Moderna) was added in a single dosage. The photo-Fenton experiments were performed in 500 mL beakers, and the variation levels were according to Table 2.

All the tests were performed in sunlight, at ambient temperature (28.4°C–30.1°C) and radiation intensity varying from $856 \text{ W}\cdot\text{m}^{-2}$ at 12 PM to $775 \text{ W}\cdot\text{m}^{-2}$ at 2 PM, measured by the Automatic Meteorological Station (Vaisala, model MAWS 301) of the Brazilian Institute of Meteorology, installed at coordinates 7°09'S, 34°48'W and an altitude of 34 m. A shaking table (Orbital SL 180/D) adjusted at 115 rpm [28] was used to achieve fast mixing. After 120 min of reaction time [25,38], the 6 M NaOH solution was added dropwise to adjust the pH to 8.0, to end the reaction and to precipitate the residual ferric ions [23,25].

Table 3
Optimisation criteria of the selected responses

Response	Symbol	Limit
COD removal	Y_1	>75%
Turbidity removal	Y_2	>90%
Colour removal	Y_3	>97%
Generation of settleable solids	Y_4	<60 mL·L ^{−1}
Generation of total solids	Y_5	<50 mg·L ^{−1}

COD, turbidity and total solids analyses were performed as previously stated on section 2.1. The samples were centrifuged at 6,000 rpm for 15 min (Novatecnica NT 825) to reduce the interference of suspended particles in the COD and colour analyses. In order to prevent the interference of the residual H_2O_2 in the COD analysis, samples were heated in a water bath at 50°C for 30 min [26]. COD was determined with a Hach (model DR 1900) spectrophotometer. The volumetric method to determine settleable solids (2540 F- Standard Methods) was adapted for this test, considering that a 50 mL sample volume was used, and then, the amount of settleable solids in 1 L of sample was estimated. The colour number (CN) defined in Eq. (3) was used to characterise the colour, based on the determination of the spectral absorption coefficient (SAC in cm^{-1}) in the visible range, at wavelengths of 436, 525 and 620 nm. The SAC was calculated for the absorbance value of a cell of thickness l (cm) with Eq. (4) [17]. The absorbance value was determined using an Agilent (model 8453) spectrophotometer.

$$CN = \frac{SAC_{436}^2 + SAC_{525}^2 + SAC_{620}^2}{SAC_{436} + SAC_{525} + SAC_{620}} \quad (3)$$

$$SAC = \frac{Abs}{l} \quad (4)$$

3. Results and discussion

3.1. Formulation of the quadratic regression models

The coded variables, their experimental values (X_1 – X_3), the reagents dosage and the observed responses (Y_1 – Y_5) are shown in Table 4. The tests performed at the central points (tests 15–18) simultaneously met all the pre-defined limits (Table 3).

The results obtained were analysed by ANOVA. Equations from the first ANOVA analysis were modified by eliminating the terms found statistically insignificant. Then, only the statistically significant terms (P-value < 0.05) were considered in the reduced quadratic model (Table 5). The coefficients of the reduced models in the polynomial expression were calculated by multiple regression analysis.

All the interactions between the variables were significant for the removal of COD, turbidity and colour, as well as for the generation of settleable solids (Table 5). It would not be possible to consider the interactions between the variables in the one-factor-at-a-time method, where the behaviour of each variable affecting the process is studied individually. This demonstrates the advantage of multivariate analysis. Amiri and Sabour [29] have studied the influence of the initial pH, $[H_2O_2]/[Fe^{2+}]$ and $[Fe^{2+}]$ in the Fenton process with the goal of maximising COD removal from landfill leachates and reported an important second

Table 4
Planning matrix and responses observed in the central composite design

Test No.	Variables					Responses				
	$[H_2O_2]$		$[FeSO_4]$		pH	Y_1	Y_2	Y_3	Y_4	Y_5
	Factor (X_1)	Value ^a ($mg \cdot L^{-1}$)	$[H_2O_2]/[FeSO_4]$ (X_2) ^b	Value ($mg \cdot L^{-1}$)	Value (X_3)	(%)	(%)	(%)	($mL \cdot L^{-1}$)	($mg \cdot L^{-1}$)
1	0.6 (–1)	2,598.9	2 (–1)	1,299.5	2.5 (–1)	74.2	84.3	93.3	120.0	68.2
2	0.6 (–1)	2,598.9	2 (–1)	1,299.5	3.5 (1)	73.7	86.3	94.6	80.0	56.2
3	0.6 (–1)	2,598.9	6 (1)	433.2	2.5 (–1)	48.7	93.3	96.4	60.0	50.2
4	0.6 (–1)	2,598.9	6 (1)	433.2	3.5 (1)	46.9	96.5	99.3	40.0	45.7
5	1.4 (1)	6,064.1	2 (–1)	3,032.1	2.5 (–1)	74.8	85.3	97.5	180.0	74.7
6	1.4 (1)	6,064.1	2 (–1)	3,032.1	3.5 (1)	76.2	88.7	99.3	100.0	68.6
7	1.4 (1)	6,064.1	6 (1)	1,010.7	2.5 (–1)	82.0	92.5	97.8	94.0	51.2
8	1.4 (1)	6,064.1	6 (1)	1,010.7	3.5 (1)	74.5	87.0	88.5	40.0	44.2
9	0.33 (1.68)	1,420.7	4 (0)	355.2	3 (0)	51.4	95.4	97.2	40.0	47.8
10	1.67 (1.68)	7,242.3	4 (0)	1,810.6	3 (0)	64.5	88.1	98.6	60.0	54.7
11	1 (0)	4,331.5	0.64 (–1.68)	6,768.0	3 (0)	78.4	59.0	95.8	150.0	117.9
12	1 (0)	4,331.5	7.36 (1.68)	588.5	3 (0)	61.8	94.1	98.4	40.0	44.6
13	1 (0)	4,331.5	4 (0)	1,082.9	2.16 (–1.68)	81.0	97.1	97.2	120.0	55.2
14	1 (0)	4,331.5	4 (0)	1,082.9	3.84 (1.68)	79.8	90.8	90.2	40.0	29.0
15	1 (0)	4,331.5	4 (0)	1,082.9	3 (0)	78.5	93.2	98.1	50.0	49.1
16	1 (0)	4,331.5	4 (0)	1,082.9	3 (0)	78.4	94.5	97.3	46.0	48.2
17	1 (0)	4,331.5	4 (0)	1,082.9	3 (0)	78.3	94.8	98.0	44.0	47.1
18	1 (0)	4,331.5	4 (0)	1,082.9	3 (0)	78.9	94.0	97.4	48.0	45.8

^a $[H_2O_2] = H_2O_2$ factor $\times 2.125 \times COD_{raw\ leachate}$ ($2,038.4 mg \cdot L^{-1}$)

^b $[H_2O_2]/[FeSO_4]$ ratio considering O_2 stoichiometric quantities necessary for total COD stabilisation.

Y_1 : COD removal, Y_2 : turbidity removal, Y_3 : colour removal, Y_4 : generation of settleable solids, Y_5 : generation of total solids.

order effect (pH \times $[\text{Fe}^{2+}]$), indicating a close correlation between the variables. This kind of correlation strengthens the need to use multivariate analyses considering that one-factor-at-a-time approach would have certainly resulted in different conclusions.

The reduced quadratic models were statistically analysed through ANOVA (Table 6). All five models were satisfactorily fitted to the experimental responses ($R^2 > 0.75$) and had P-values lower than 0.05, indicating the significance of the regressions. However, turbidity and colour removal models presented low predictability (with $F_{\text{value}}/F_{\text{table}}$ less than 4) and Adj. $R^2 < 0.75$, which could be explained by the weak relations between experimental variables and such responses. Even with this lack of fit, the models have been validated experimentally in this work (section 3.3).

3.2. Simultaneous optimisation of the responses and optimal conditions

3.2.1. H_2O_2 factor and pH

The contour plots of the interaction between the H_2O_2 factor (X_1) and pH (X_3) are shown in Fig. 1. The intersection between the contour plots according to the pre-defined limits (Table 3) was obtained to determine the optimal region (in grey, Fig. 2).

It was observed (Fig. 2) that COD removal and the generation of total solids were responsible for the delimitation of the ideal H_2O_2 concentration. A lack of H_2O_2 would result in insufficient production of $\bullet\text{OH}$ to oxidise the organic matter; on the other hand, an excess of H_2O_2 would promote reactions that sequester $\bullet\text{OH}$ radical, reducing the pollutant degradation rate, which inhibits the removal process [23]. In addition,

Table 5
Regression models in terms of decoded variables

Response	Proposed quadratic model
Y_1	$Y(X) = 58.37 + 77.66X_1 - 1.99X_2 - 9.87X_3 - 45.51X_1^2 - 0.75X_2^2 + 2.63X_3^2 + 9.05X_1X_2 - 2.36X_1X_3 - 1.27X_2X_3$
Y_2	$Y(X) = 53.86 + 6.11X_1 + 17.50X_2 - 1.43X_2^2 - 2.14X_1X_2 - 0.35X_1X_3 - 0.28X_2X_3$
Y_3	$Y(X) = 57.84 + 28.68X_3 - 5.70X_3^2 - 1.26X_1X_2 + 1.66X_1X_3 + 0.41X_2X_3$
Y_4	$Y(X) = 748.55 + 147.30X_1 - 65.22X_2 - 370.10X_3 + 23.61X_1^2 + 4.92X_2^2 + 57.54X_3^2 - 7.19X_1X_2 - 46.25X_1X_3 + 5.75X_2X_3$
Y_5	$Y(X) = 49.71 + 17.55X_1 - 27.06X_2 + 48.25X_3 + 2.85X_2^2 - 9.84X_3^2 - 3.02X_1X_2$

X_1 : H_2O_2 factor, X_2 : $[\text{H}_2\text{O}_2]/[\text{FeSO}_4]$ ratio, X_3 : pH.

Y_1 : COD removal, Y_2 : turbidity removal, Y_3 : colour removal, Y_4 : generation of settleable solids, Y_5 : generation of total solids.

Table 6
ANOVA chart of the response models

Response	Source of variation	Sum of squares	Degrees of freedom	Mean square	F_{value}	F_{table}	$F_{\text{value}}/F_{\text{table}}$	R^2	Adj. R^2	P-value
Y_1	Regression	2,175.14	9	241.68	28.55	3.39	8.42	0.970	0.936	<0.0001
	Residual	67.72	8	8.47						
	Total	2,242.87								
Y_2	Regression	1,023.39	6	170.57	7.80	3.09	2.52	0.810	0.706	<0.01
	Residual	240.68	11	21.88						
	Total	1,264.08								
Y_3	Regression	114.42	5	22.88	7.44	3.11	2.39	0.756	0.654	<0.01
	Residual	36.91	12	3.08						
	Total	151.33								
Y_4	Regression	30,672.77	9	3,408.09	35.45	3.39	10.46	0.976	0.948	<0.0001
	Residual	769.01	8	96.13						
	Total	31,441.78								
Y_5	Regression	5,406.51	6	901.09	16.71	3.09	5.41	0.901	0.847	<0.0001
	Residual	593.07	11	53.92						
	Total	5,999.58								

Y_1 : COD removal, Y_2 : turbidity removal, Y_3 : colour removal, Y_4 : generation of settleable solids, Y_5 : generation of total solids.

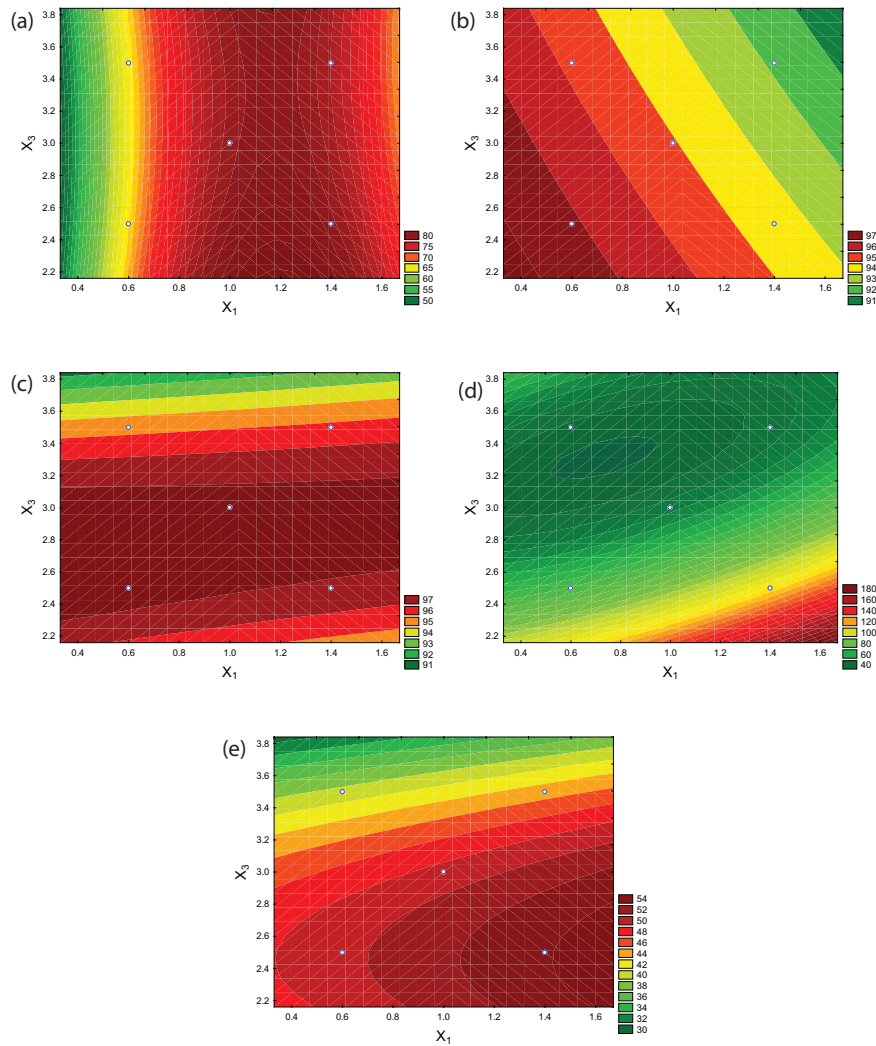


Fig. 1. Contour plots as a function of the H_2O_2 factor (X_1) and pH (X_3) for the responses: (a) COD removal (Y_1), (b) turbidity removal (Y_2), (c) colour removal (Y_3), (d) generation of settleable solids (Y_4) and (e) generation of total solids (Y_5). Reagents ratio (X_2) = 4.

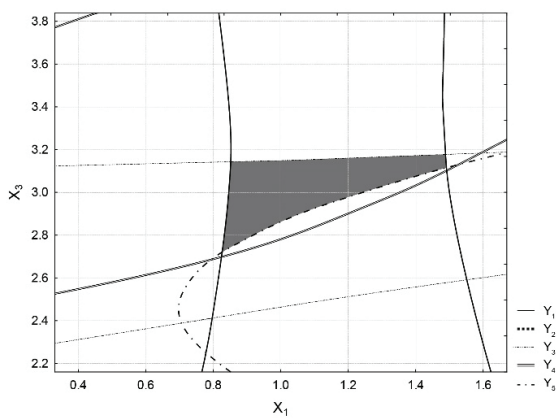


Fig. 2. Optimal region of the following variables: H_2O_2 factor (X_1) and pH (X_3) Reagents ratio (X_2) = 4. All variables are in decoded form. Y_1 : COD removal >75%, Y_2 : turbidity removal >90%, Y_3 : colour removal >97%, Y_4 : generation of settleable solids <60 $mL \cdot L^{-1}$, Y_5 : generation of total solids <50 $mg \cdot L^{-1}$.

it was observed that a pH between 3.11 and 3.15 favoured a wider range of the H_2O_2 factor. To explain this behaviour, it is assumed that this pH range enables faster reactions between $[Fe(H_2O)]^{2+}$ and H_2O_2 , reduces the sequestration of $\bullet OH$ radicals by the H^+ ions, favours the reactions between Fe^{3+} and H_2O_2 , and propitiates the predominance of more photoreactive iron complexes [36]. Assuming that sludge is formed from the precipitation of Fe^{3+} as iron oxy-hydroxides [39], this explains how pH and a H_2O_2 concentration out of that range resulted in higher sludge generation and lower oxidation efficiency.

Regarding the ideal pH, COD removal and total solids removal delimited the lower limit, while the COD and colour removal delimited the upper limit. This can be attributed to the effective role of the pH range in the oxidation of organic matter, not just its coagulation, which resulted in less sludge generation [29], reduction of the supernatant's COD, and higher removal or transformation of the compounds that give colour to the effluent. The removal of the leachate's colour can be attributed to the

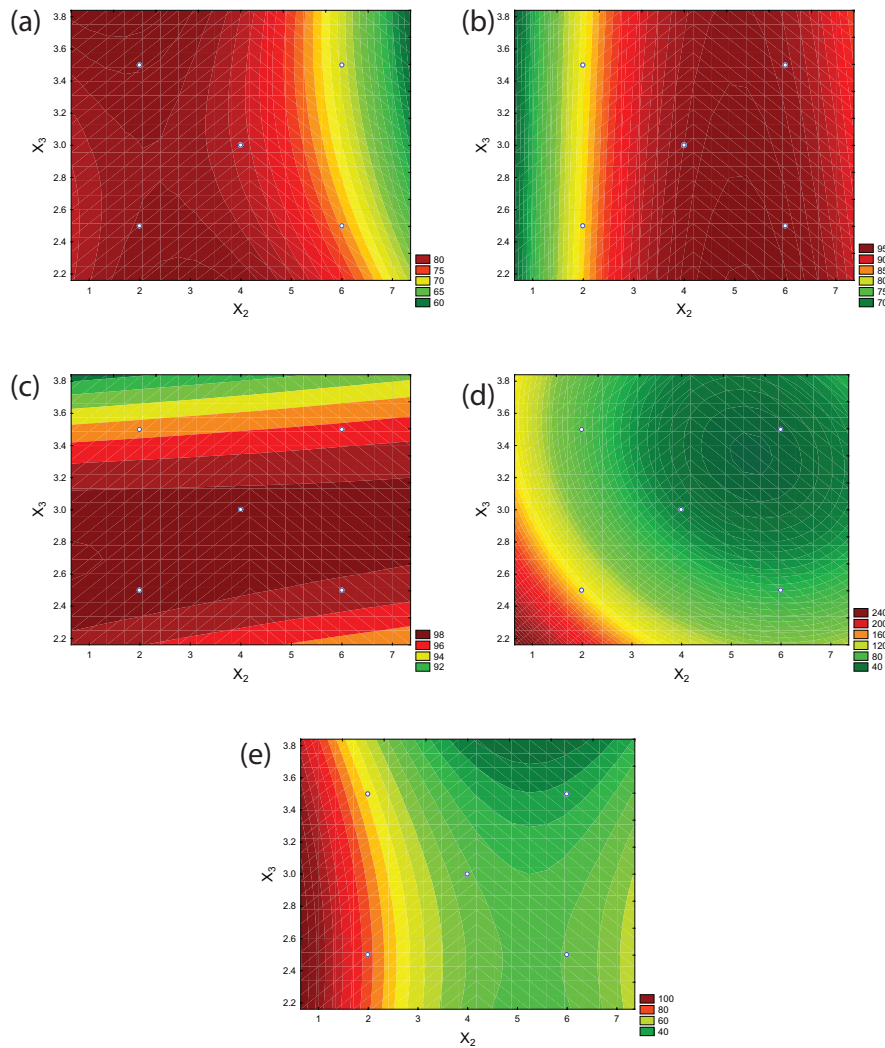


Fig. 3. Contour plots as a function of the reagents ratio (X_2) and pH (X_3) for the responses: (a) COD removal (Y_1), (b) turbidity removal (Y_2), (c) colour removal (Y_3), (d) generation of settleable solids (Y_4) and (e) generation of total solids (Y_5). H_2O_2 factor (X_1) = 1.

elimination of humic substances responsible for the strong brown colour of leachates [11], which demonstrates the capability of the photocatalytic process to remove compounds that colour the effluent.

3.2.2. Reagents ratio and pH

The contour plots of the interaction between the reagents ratio (X_2) and pH (X_3) are shown in Fig. 3. The optimal region resulted from the intersection between the contour plots (Fig. 4).

COD removal and generation of settleable solids simultaneously delimited the maximum reagents ratio and the minimum pH (Fig. 4). In fact, a very low pH had negative effects on the Fenton reaction, and low iron concentrations relative to H_2O_2 concentrations resulted in insufficient generation of $\bullet OH$ radicals, increased reaction time, propitiated a high H_2O_2 residue level, and contributed to the sequestration of $\bullet OH$ radicals by the excess H_2O_2 [36]. The lower limit of the reagents ratio was defined by the colour removal and

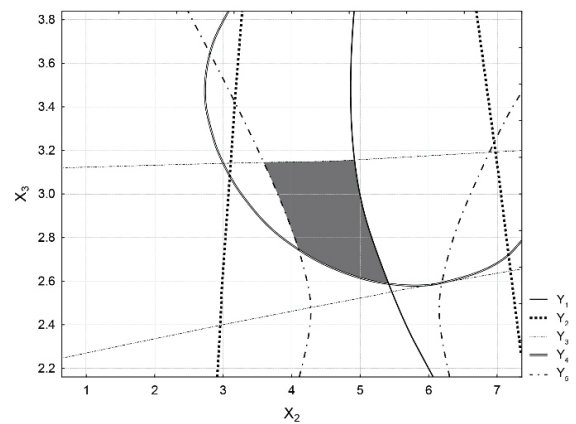


Fig. 4. Optimal region of the following variables: reagents ratio (X_2) and pH (X_3); H_2O_2 factor (X_1) = 1. All variables are in decoded form. Y_1 : COD removal >75%, Y_2 : turbidity removal >90%, Y_3 : colour removal >97%, Y_4 : generation of settleable solids <60 $mL \cdot L^{-1}$, Y_5 : generation of total solids <50 $mg \cdot L^{-1}$.

generation of total solids. It must be highlighted that excess iron contributes to the increase of sludge generation caused by the precipitation of iron oxy-hydroxides, mainly at a high pH [40], in addition to favouring $\bullet\text{OH}$ sequestration [36], which results in a reduction of the compounds' degradation efficiency, particularly of those related to the leachate colour. Amiri and Sabour [29] have emphasised the importance of an optimal reagents ratio, considering that when this is not achieved, $\bullet\text{OH}$ radical sequestration reactions may occur because of the excess of one of the reagents, and this reduces the pollutants' removal rate and inhibits the process.

pH was delimited on the upper side (Fig. 4) by COD and colour removal, while its lower limit was determined by the COD removal and the generation of settleable solids, which demonstrates the importance of these responses for defining the initial pH of the reaction, as discussed in the previous section.

3.2.3. H_2O_2 factor and reagents ratio

The contour plots of the interaction between the H_2O_2 factor (X_1) and the reagents ratio (X_2) are shown in Fig. 5. The optimal region results of the intersection of the contour plots are presented in Fig. 6.

The upper limit of the H_2O_2 factor was determined by COD and colour removal (Fig. 6). High H_2O_2 concentration reduces the removal of organic matter and effluent colour because of the combination of excess H_2O_2 with $\bullet\text{OH}$ radicals [25]. The upper limit of the reagents ratio was defined by the removal of COD and colour. In fact, $[\text{H}_2\text{O}_2]/[\text{FeSO}_4]$ ratios above the optimal region affected the removal of organic matter and colour because of the lack of catalyst and the excess of H_2O_2 , which hindered the generation of radicals that oxidise organic matter.

COD removal and generation of total solids determined the minimum values of the H_2O_2 factor and the reagents ratio

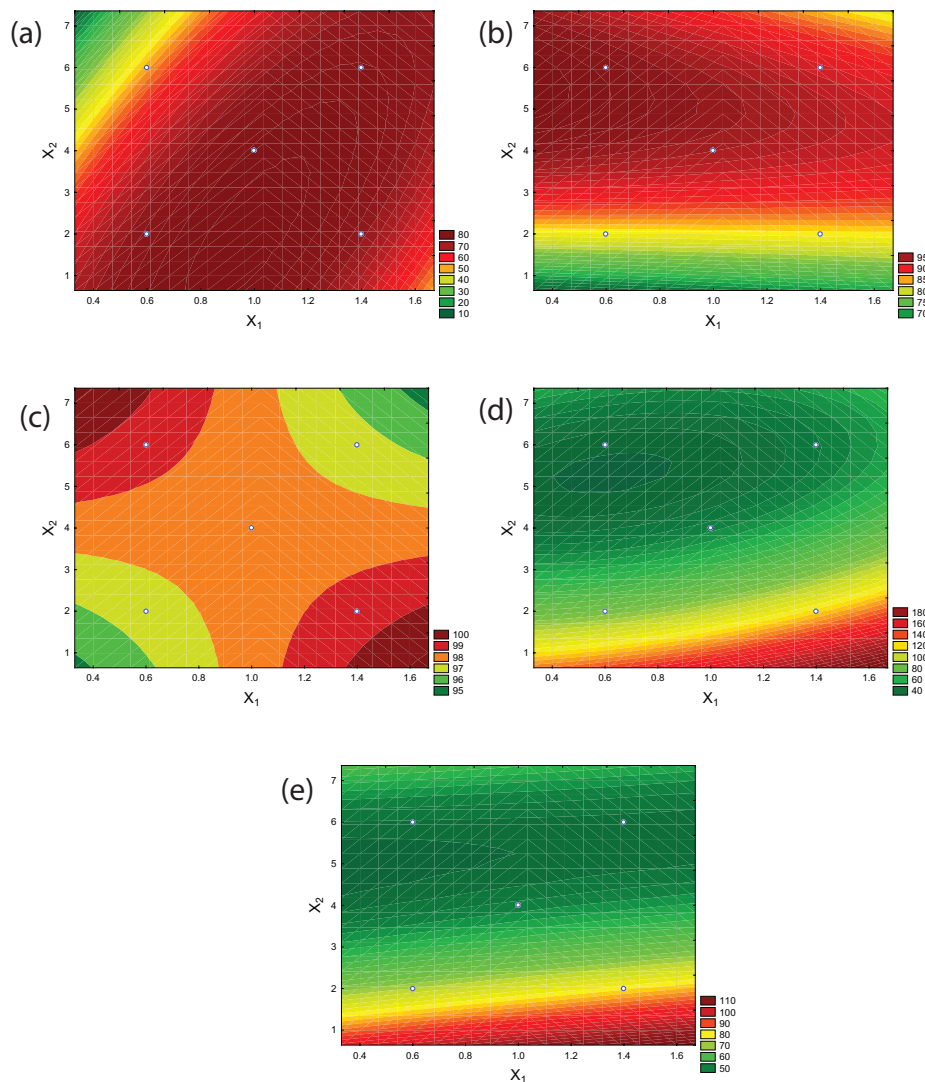


Fig. 5. Contour plots as a function of H_2O_2 factor (X_1) and reagents ratio (X_2) for the responses: (a) COD removal (Y_1), (b) turbidity removal (Y_2), (c) colour removal (Y_3), (d) generation of settleable solids (Y_4) and (e) generation of total solids (Y_5). pH (X_3) = 3.

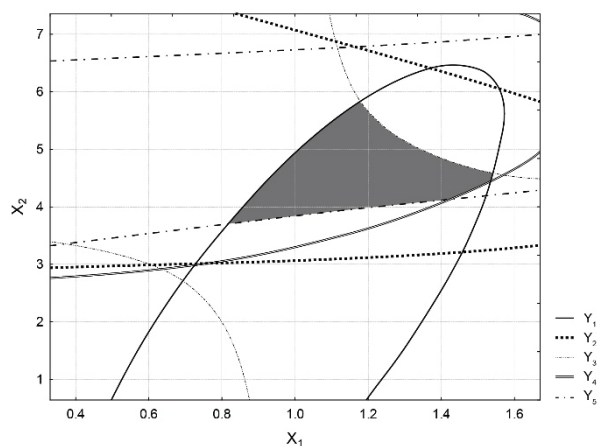


Fig. 6. Optimal region of the following variables: H_2O_2 factor (X_1) and reagents ratio (X_2); pH (X_3) = 3. All variables are in decoded form. Y_1 : COD removal >75%, Y_2 : turbidity removal >90%, Y_3 : colour removal >97%, Y_4 : generation of settleable solids <60 $\text{mL}\cdot\text{L}^{-1}$, Y_5 : generation of total solids <50 $\text{mg}\cdot\text{L}^{-1}$.

at the same time. Very low H_2O_2 concentrations combined with relatively high iron concentrations were not the ideal conditions to maximise the generation of $\bullet\text{OH}$ radicals, which hindered the removal of organic compounds and favoured higher formation of sludge. In addition, higher than the ideal $\text{Fe}^{2+}/\text{COD}$ ratios do not result in a significant increase of the COD removal, do not increase the pollutant degradation rates, and cause higher sludge generation [17].

3.2.4. Optimal ranges of the variables

The optimal ranges of the variables (Table 7) were determined from the overlay of the contour plots (Figs. 2, 4 and 6), considering the most restricted values.

The ideal range of the H_2O_2 factor varied between 83% and 150% of the H_2O_2 amount relative to the stoichiometric quantity of O_2 necessary to totally stabilise COD. In other words, the ideal H_2O_2 range varied between 1.764 and 3.188 g of H_2O_2 per g of COD of initial leachate in the process. The ideal $[\text{H}_2\text{O}_2]/[\text{FeSO}_4]$ ratio ranged from 3.7 to 5.4, which is $[\text{H}_2\text{O}_2]/[\text{Fe}^{2+}]$ molar ratio between 30.24 and 44.13, in accordance with previously reported values in the literature [36]. Kim and Vogelpohl [41] have reported the use of $[\text{H}_2\text{O}_2]/[\text{Fe}^{2+}]$ molar ratios of 26.2 and 35.0 for the photo-Fenton and photo-Fenton-like processes, respectively. These values are significantly higher than those used in the conventional Fenton process, which results in lower use of iron, lower costs, and reduction of sludge generation. Moreover, the optimal pH range was in accordance with the values adopted for the photo-Fenton process [42,43]. It is important to be mentioned that the operational conditions of the variables under study are intrinsically related, so they must be determined together through the optimal region graphs (Figs. 2, 4 and 6), which stresses the importance of multivariate process optimisation. Finally, extra tests were conducted within the optimal range of the variables to confirm if the results were in agreement with the values predicted by the models.

Table 7

Critical range for each variable under study

Variable	Critical range
H_2O_2 factor	$0.83 \leq X_1 \leq 1.50$
$[\text{H}_2\text{O}_2]/[\text{FeSO}_4]$	$3.70 \leq X_2 \leq 5.40$
pH	$2.72 \leq X_3 \leq 3.15$

Table 8

Validation tests under the optimal conditions based on the overlay plots

Response	Test No.	Actual	Calculated	Error (%)	SD ^a ($\pm\%$)
COD removal (%)	1	75.4	78.7	4.3	2.4
	2	74.4	78.7	5.5	3.0
	3	75.5	78.7	4.0	2.2
Turbidity removal (%)	1	90.9	94.2	3.6	2.4
	2	92.7	94.2	1.6	1.1
	3	93.2	94.2	1.1	0.8
Colour removal (%)	1	99.1	97.6	1.5	1.0
	2	99.1	97.6	1.6	1.1
	3	98.1	97.6	0.5	0.4
Settleable solids ($\text{mL}\cdot\text{L}^{-1}$)	1	54.0	51.8	4.3	1.6
	2	50.0	51.8	3.4	1.3
	3	50.0	51.8	3.4	1.3
Total solids ($\text{mg}\cdot\text{L}^{-1}$)	1	48.1	49.7	3.1	1.1
	2	49.4	49.7	0.7	0.2
	3	48.9	49.7	1.7	0.6

^aSD: Standard deviation

3.3. Experimental validation

Three tests were performed to validate the optimisation process under the following conditions suggested by the overlay plots: H_2O_2 factor = 1, $[\text{H}_2\text{O}_2]/[\text{FeSO}_4] = 4$, and initial pH of ~2.9. The results of the experiments were compared with the values calculated by the models, as shown in Table 8. The error between the calculated and the experimental values varied between 0.5% and 5.5% with a standard deviation between 0.2% and 3.0%, probably because of non-controllable process variables, such as reaction temperature and incidence of solar radiation. The results show that the model can be reproduced within the studied range and that the optimisation process can be considered valid.

4. Conclusion

An investigation on a real municipal solid waste landfill leachate was conducted to analyse the effectiveness of the solar photo-Fenton process as a post-treatment stage, applying CCD and RSM in order to develop a predictive model and to determine the optimal conditions. The following results were obtained out of this study:

- Solar photo-Fenton process as a post-treatment method proved to be effective in removing recalcitrant organic

compounds (>75%), turbidity (>90%) and colour (>97%) in a mature landfill leachate.

- A disadvantage of the photo-Fenton reaction was mitigated by the optimisation of the process in order to minimise sludge production, resulting in a generation of settleable solids <60 mL·L⁻¹ and generation of total solids <50 mg·L⁻¹.
- The statistical analysis of the proposed quadratic models seemed adequate. Since turbidity and colour removal models presented the weakest relations between experimental variables and such responses, the models have been validated experimentally.
- Operational conditions of the variables under study are intrinsically related, so they must be determined through the optimal region graphs. By the overlay plots, the relevance of a multi-response optimisation was demonstrated. Consequently, factorial design using a univariate approach or adopting a single response are incomplete and can lead to inconsistent results.
- To reduce the adverse environmental impacts and costs related to the photo-Fenton process, sunlight was used to potentiate degradation reactions, and two new sludge production responses were minimised (generation of settleable and total solids). It is suggested that other alternatives are researched on bench, pilot and real scale to make the process more sustainable, and to improve the performance of this process.

Acknowledgement

The authors thank the Brazilian Coordination for the Improvement of Higher Education Personnel (CAPES) for financial support, the technicians from the Sanitation Laboratory at the Federal University of Paraíba for the experimental analysis support, the João Pessoa Municipal Urban Cleaning Company (EMLUR) for providing landfill leachate samples, and the researchers Rennio Felix de Sena and Fernando Fernandes Vieira for their valuable assistance in revising the text. Special thanks to the Federal University of Paraíba for the opportunity to develop the research, publishing support, and language editing.

Symbols

Abs	–	Absorbance value
β_0	–	Intercept constant
β_i	–	Coefficient of the first order term of factor i
β_{ii}	–	Coefficient of the quadratic term of factor i
β_{ij}	–	Interaction coefficient between factors i and j
CN	–	Colour number
ε	–	Residue
k	–	Number of variables
l	–	Thickness, cm
R^2	–	Determination coefficient
SAC	–	Spectral absorption coefficient, cm ⁻¹
X_i and X_j	–	Decoded values of the factors
Y	–	Response

References

- [1] X. Wu, H. Zhang, Y. Li, D. Zhang, X. Li, Factorial design analysis for COD removal from landfill leachate by

- photo-assisted Fered-Fenton process, *Environ. Sci. Pollut. Res.*, 21 (2014) 8595–8602.
- [2] T.H. Christensen, P. Kjeldsen, P.L. Bjerg, D.L. Jensen, J.B. Christensen, A. Baun, H.-J. Albrechtsen, G. Heron, Biogeochemistry of landfill leachate plumes, *Appl. Geochem.*, 16 (2001) 659–718.
- [3] T.H. Christensen, P. Kjeldsen, H. Albrechtsen, G. Heron, P.H. Nielsen, P.L. Bjerg, P.E. Holm, Attenuation of landfill leachate pollutants in aquifers, *Crit. Rev. Environ. Sci. Technol.*, 24 (1994) 119–202.
- [4] V.J.P. Vilar, T.F.C.V. Silva, M.A.N. Santos, A. Fonseca, I. Saraiva, R.A.R. Boaventura, Evaluation of solar photo-Fenton parameters on the pre-oxidation of leachates from a sanitary landfill, *Sol. Energy*, 86 (2012) 3301–3315.
- [5] S. Mukherjee, S. Mukhopadhyay, M.A. Hashim, B. Sen Gupta, contemporary environmental issues of landfill leachate: assessment and remedies, *Crit. Rev. Environ. Sci. Technol.*, 45 (2015) 472–590.
- [6] N. Meky, M. Fujii, C. Yoshimura, A. Tawfik, Feasibility of using non-vegetated baffled submerged constructed wetland system for removal of heavy metals, COD and nutrients from hyper-saline hazardous landfill leachate, *Desal. Wat. Treat.*, 98 (2017) 254–265.
- [7] E. Neczaj, M. Kacprzak, J. Lach, E. Okoniewska, Effect of sonication on combined treatment of landfill leachate and domestic sewage in SBR reactor, *Desalination*, 204 (2007) 227–233.
- [8] T. Robinson, Removal of toxic metals during biological treatment of landfill leachates, *Waste. Manage.*, 63 (2017) 299–309.
- [9] Z.-L. Ye, Y. Hong, S. Pan, Z. Huang, S. Chen, W. Wang, Full-scale treatment of landfill leachate by using the mechanical vapor recompression combined with coagulation pretreatment, *Waste Manage.*, 66 (2017) 88–96.
- [10] J. Hashisho, M. El-Fadel, M. Al-Hindi, D. Salam, I. Alameddine, Hollow fiber vs. flat sheet MBR for the treatment of high strength stabilized landfill leachate, *Waste. Manage.*, 55 (2016) 249–256.
- [11] T.F.C.V. Silva, R. Ferreira, P.A. Soares, D.R. Manenti, A. Fonseca, I. Saraiva, R.A.R. Boaventura, V.J.P. Vilar, Insights into solar photo-Fenton reaction parameters in the oxidation of a sanitary landfill leachate at lab-scale, *J. Environ. Manage.*, 164 (2015) 32–40.
- [12] T.F.C.V. Silva, A. Fonseca, I. Saraiva, R.A.R. Boaventura, V.J.P. Vilar, Scale-up and cost analysis of a photo-Fenton system for sanitary landfill leachate treatment, *Chem. Eng. J.*, 283 (2016) 76–88.
- [13] E. Neyens, J. Baeyens, A review of classic Fenton's peroxidation as an advanced oxidation technique, *J. Hazard. Mater.*, 98 (2003) 33–50.
- [14] A. Koltsakidou, M. Antonopoulou, M. Sykiotou, E. Evgenidou, I. Konstantinou, D.A. Lambropoulou, Photo-Fenton and Fenton-like processes for the treatment of the antineoplastic drug 5-fluorouracil under simulated solar radiation, *Environ. Sci. Pollut. Res.*, 24 (2017) 4791–4800.
- [15] T.A. Kurniawan, W. Lo, G.Y.S. Chan, Radicals-catalyzed oxidation reactions for degradation of recalcitrant compounds from landfill leachate, *Chem. Eng. J.*, 125 (2006) 35–57.
- [16] L. Prieto-Rodríguez, D. Spasiano, I. Oller, I. Fernández-Calderero, A. Agüera, S. Malato, Solar photo-Fenton optimization for the treatment of MWTP effluents containing emerging contaminants, *Catal. Today*, 209 (2013) 188–194.
- [17] O. Primo, M.J. Rivero, I. Ortiz, Photo-Fenton process as an efficient alternative to the treatment of landfill leachates, *J. Hazard. Mater.*, 153 (2008) 834–842.
- [18] E.M.R. Rocha, V.J.P. Vilar, A. Fonseca, I. Saraiva, R.A.R. Boaventura, Landfill leachate treatment by solar-driven AOPs, *Sol. Energy*, 85 (2011) 46–56.
- [19] M.C.V.M. Starling, P.H.R. dos Santos, F.A.R. de Souza, S.C. Oliveira, M.M.D. Leão, C.C. Amorim, Application of solar photo-Fenton toward toxicity removal and textile wastewater reuse, *Environ. Sci. Pollut. Res.*, 24 (2017) 12515–12528.
- [20] R.L. Mason, R.F. Gunst, J.L. Hess, *Statistical Design and Analysis of Experiments*, John Wiley & Sons, Inc., Hoboken, 2003.

- [21] R.H. Myers, D.C. Montgomery, C.M. Anderson-Cook, *Response Surface Methodology: Process and Product Optimization Using Designed Experiments*, 4th ed., John Wiley & Sons, Hoboken, 2016.
- [22] H. Zhang, H.J. Choi, P. Canazo, C. Huang, Multivariate approach to the Fenton process for the treatment of landfill leachate, *J. Hazard. Mater.*, 161 (2009) 1306–1312.
- [23] Y. Wu, S. Zhou, F. Qin, X. Ye, K. Zheng, Modeling physical and oxidative removal properties of Fenton process for treatment of landfill leachate using response surface methodology (RSM), *J. Hazard. Mater.*, 180 (2010) 456–465.
- [24] H. Li, S. Zhou, Y. Sun, J. Lv, Application of response surface methodology to the advanced treatment of biologically stabilized landfill leachate using Fenton's reagent, *Waste Manage.*, 30 (2010) 2122–2129.
- [25] S. Mohajeri, H.A. Aziz, M.A. Zahed, L. Mohajeri, M.J.K. Bashir, S.Q. Aziz, M.N. Adlan, M.H. Isa, Multiple responses analysis and modeling of Fenton process for treatment of high strength landfill leachate, *Water. Sci. Technol.*, 64 (2011) 1652–1660.
- [26] M. Ghanbarzadeh Lak, M.R. Sabour, A. Amiri, O. Rabbani, Application of quadratic regression model for Fenton treatment of municipal landfill leachate, *Waste. Manage.*, 32 (2012) 1895–1902.
- [27] A. Talebi, N. Ismail, T.T. Teng, A.F.M. Alkarkhi, Optimization of COD, apparent color, and turbidity reductions of landfill leachate by Fenton reagent, *Desal. Wat. Treat.*, 52 (2014) 1524–1530.
- [28] W.G. Moravia, M.C.S. Amaral, L.C. Lange, Evaluation of landfill leachate treatment by advanced oxidative process by Fenton's reagent combined with membrane separation system, *Waste. Manage.*, 33 (2013) 89–101.
- [29] A. Amiri, M.R. Sabour, Multi-response optimization of Fenton process for applicability assessment in landfill leachate treatment, *Waste. Manage.*, 34 (2014) 2528–2536.
- [30] H.S. Erkan, O. Apaydin, Final treatment of young, middle-aged, and stabilized leachates by Fenton process: optimization by response surface methodology, *Desal. Wat. Treat.*, 54 (2015) 342–357.
- [31] M.R. Sabour, A. Amiri, Comparative study of ANN and RSM for simultaneous optimization of multiple targets in Fenton treatment of landfill leachate, *Waste. Manage.*, 65 (2017) 54–62.
- [32] G.C. Heng, E.S. Elmolla, M. Chaudhuri, Optimization of photo-fenton treatment of mature landfill leachate, *Nat. Environ. Pollut. Technol.*, 11 (2012) 65–72.
- [33] APHA/AWWA/ WEF, *Standard Methods for the Examination of Water and Wastewater*, 22nd ed., American Public Health Association (APHA), Washington, DC., 2012.
- [34] Y.W. Kang, K.Y. Hwang, Effects of reaction conditions on the oxidation efficiency in the Fenton process, *Water. Res.*, 34 (2000) 2786–2790.
- [35] S. Kim, S. Geissen, A. Vogelpohl, Landfill leachate treatment by a photo-assisted Fenton reaction, *Water. Sci. Technol.*, 35 (1997) 239–248.
- [36] Y. Deng, D. Englehardt, Treatment of landfill leachate by the Fenton process, *Water. Res.*, 40 (2006) 3683–3694.
- [37] Y. Deng, Physical and oxidative removal of organics during Fenton treatment of mature municipal landfill leachate, *J. Hazard. Mater.*, 146 (2007) 334–340.
- [38] Y. Wu, S. Zhou, F. Qin, H. Peng, Y. Lai, Y. Lin, Removal of humic substances from landfill leachate by Fenton oxidation and coagulation, *Process. Saf. Environ. Prot.*, 88 (2010) 276–284.
- [39] S. Papoutsakis, C. Pulgarin, I. Oller, R. Sánchez-Moreno, S. Malato, Enhancement of the Fenton and photo-Fenton processes by components found in wastewater from the industrial processing of natural products: the possibilities of cork boiling wastewater reuse, *Chem. Eng. J.*, 304 (2016) 890–896.
- [40] N. Kishimoto, T. Kitamura, M. Kato, H. Otsu, Reusability of iron sludge as an iron source for the electrochemical Fenton-type process using Fe²⁺/HOCl system, *Water. Res.*, 47 (2013) 1919–1927.
- [41] S-M. Kim, A. Vogelpohl, Degradation of Organic Pollutants by the Photo-Fenton-Process, *Chem. Eng. Technol.*, 21 (1998) 187–191.
- [42] T.F.C.V. Silva, M.E.F. Silva, A. Cristina Cunha-Queda, A. Fonseca, I. Saraiva, R.A.R. Boaventura, V.J.P. Vilar, Sanitary landfill leachate treatment using combined solar photo-Fenton and biological oxidation processes at pre-industrial scale, *Chem. Eng. J.*, 228 (2013) 850–866.
- [43] M. Mohadesi, A. Shokri, Evaluation of Fenton and photo-Fenton processes for the removal of p-chloronitrobenzene in aqueous environment using Box-Behnken design method, *Desal. Wat. Treat.*, 81 (2017) 199–208.